STRUCTURE DETERMINATION OF LIPID BILAYERS

C. R. WORTHINGTON AND R. S. KHARE, *Departments of Biological Sciences and Physics, Carnegie-Mellon University, Pittsburgh, Pennsylvania 15213 U.S.A.*

ABSTRACT A method of determining the phases of X-ray reflections from oriented model membrane systems at low resolution is described. The method involves deconvolution and requires that $d \geq 2v$ where v is the width of the head group region within the bilayer and d is the thickness of the bilayer. The method can be used with a single set of X-ray data and applies to lipid bilayers which have a relatively constant density in the hydrocarbon region. Phases for the first five or six orders of phosphatidylethanolamine and lecithin are derived. A refined analysis based upon deconvolution but using information inherent in the Fourier profile is also described.

INTRODUCTION

The study of the molecular structure of lipid bilayers is of current interest in that structural information derived from model membrane systems might be relevant to our understanding of the structure and function of biological membranes. Model membranes can be prepared as oriented multilayers and when examined by X-ray diffraction the regular stacking of the bilayers gives rise to a series of discrete X-ray reflections. The structure analysis of the lamellar diffraction is associated with obtaining the phases of the diffraction orders. The one-dimensional electron density profile of the membrane as a function of depth can be computed once the phases are assigned. Lipid bilayers are centrosymmetrical so that the phases (or signs) can only be + or − for each order of diffraction. The phase problem for model membrane systems refers to the finding of the correct set of phases from the 2^h possible sets, where h is the number of diffraction orders.

Electron density profiles for a number of model membrane systems have been presented (1, 2). In these studies (1, 2) the phases were obtained in a variety of ways. In some cases, phases can be directly obtained, for instance, if heavy atoms can be chemically attached to the head group (3). Direct methods of structure analysis (4, 5) can be used if the preparation contains only a few lipid bilayers (6, 7), or if the autocorrelation function of the lipid bilayer can be found by swelling (4). In the X-ray study of model membranes these three situations do not often arise because most preparations contain many layers and no heavy atoms. The swelling method (1, 2, 4) is not often used with model membranes primarily because not all lipid bilayers swell appreciably. One drawback with the swelling method is that the lipid bilayer often changes structure with swelling (2, 8, 9). In this paper we treat the case in which the model membrane system

contains many layers and no heavy atoms and for which swelling data are not available. Our analysis applies to a single set of X-ray data. In earlier work on this kind of model membrane system, phases were assigned indirectly either using model comparisons (2, 10) or by analogy to known structures (11). We report, however, that the phases can be obtained on the assumption that the lipid chains in the central part of the bilayer have uniform electron density.

The present method is related to the deconvolution method (5) which has been used to analyze X-ray data from swollen membrane systems including retinal photoreceptors (12) and nerve myelin (13).

THEORY OF METHOD

The present method as applied to lipid bilayers uses deconvolution. The diffraction theory of the deconvolution method has been previously described (5, 14) and only a brief account is given here. An attempt is made to retain the previous notations (5, 10) where possible.

Let $t(x)$ represent the electron density distribution in a direction at right angles to the membrane surface and let $T(X)$ represent its Fourier transform. Denote $t(x) \rightleftharpoons T(X)$ where $t(x)$ and $T(X)$ are a Fourier transform pair and where x, X are real and reciprocal space coordinates (10). Discrete X-ray reflections are recorded from lipid multilayers at $X = h/d$, where h is the order of diffraction and d is the unit cell dimension. Corrected intensities $J_{obs}(h)$ are obtained from the X-ray intensities (10). The notation $KJ_{obs}(h) = J(h) = |T(h)|^2$ is retained where K is the normalization constant.

The electron density $t(x)$ refers to the lipid bilayer and the origin is chosen at the center of contact of the head groups. The head group of the lipid molecule has electron density $h(x)$ and has width $v/2$ measured from $x = 0$ to the beginning of the lipid hydrocarbon chain. We first assume that L, the electron density of the hydrocarbon region, is a constant. This model for $t(x)$ is shown in Fig. 1 A. The minus L model is defined as

$$\Delta t(x) = t(x) - L, \tag{1}$$

where L is the constant density of the hydrocarbon chain region. A drawing of this model is shown in Fig. 1 B. The Fourier transform of $\Delta t(x)$ is denoted $\Delta T(X)$ and the notation $\Delta J(X) = |\Delta T(X)|^2$ is retained. The relation between $T(X)$ and $\Delta T(X)$ is

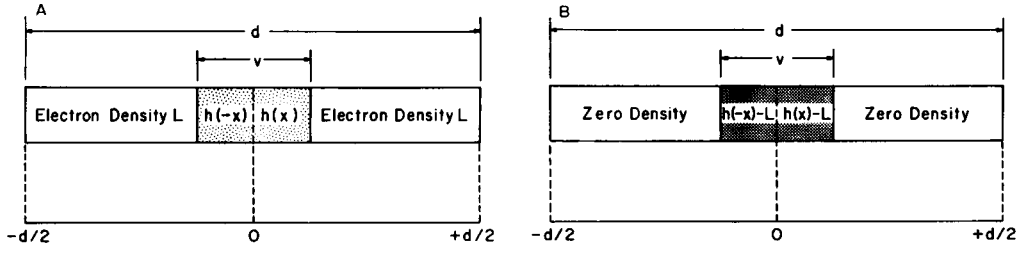

FIGURE 1 (A) Electron density model $t(x)$ for the lipid bilayer contains head group density $h(x)$ and hydrocarbon chain density L. The origin is chosen at the interface of the head group region which has width v. (B) The minus L electron density model $\Delta t(x)$ has head group density $h(x) - L$ and zero density outside of the head group region.

$$\Delta T(X) = T(X) - Ld \operatorname{sinc} \pi dX, \tag{2}$$

where $\operatorname{sinc} \theta = \sin \theta/\theta$. Hence, $\Delta T(h) = T(h)$ provided h is a nonzero integer. This means that there is no way to distinguish between the two models on the basis of the X-ray data $J_{obs}(h)$ unless the $h = 0$ reflection is recorded (10).

The deconvolution method refers to a deconvolution of the autocorrelation function $A(x)$ and $A(x)$ is defined by

$$A(x) = t(x) * t(-x), \tag{3}$$

where $*$ is the convolution symbol. In terms of the minus L model the autocorrelation function $\Delta A(x)$ is given by

$$\Delta A(x) = \Delta t(x) * \Delta t(-x). \tag{4}$$

The Patterson function $P''(x)$ for both models is given by

$$P''(x) = 2/d \sum_{1}^{h} J_{obs}(h) \cos 2\pi hx/d. \tag{5}$$

The Patterson function $P''(x)$ is shown in Fig. 2 A for the case when v lies within the range of 0 to $d/2$. $\Delta A(x)$, the autocorrelation function of the minus L model, can be obtained from the Patterson function by shifting the base line so that $\Delta A(v) = 0$ (5), and this can be done provided that $d > 2v$. The autocorrelation function $\Delta A(x)$ and the Patterson function $P''(x)$ of Eq. 5 are not on the same scale but are related (5):

$$\Delta A(x) = K[P''(x) - P''(v)], \tag{6}$$

where K is the normalization constant.

The first step in the deconvolution method is to choose the parameter v. From Figs. 2 A and B the parameter v can be directly obtained from the Patterson function when L is a constant,

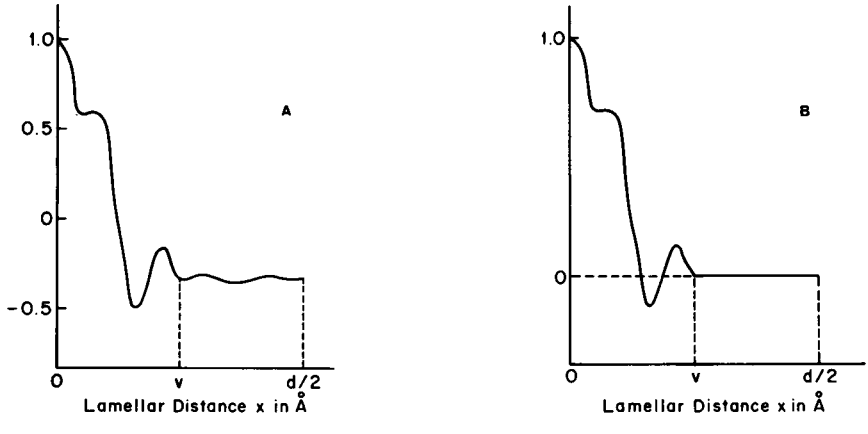

FIGURE 2 (A) The Patterson function $P''(x)$ for a hypothetical lipid bilayer has a flat region between $x = v$ and $x = d/2$. (B) The autocorrelation function $\Delta A(x)$ is obtained from A by drawing the base line in at $x = v$ such that $\Delta A(v) = 0$.

and when $d > 2v$. In practice, the choice of v might be obscured by the series termination ripple superimposed on the Patterson function or by reason that L might not be constant. The correctness of the choice of v can be examined by computing $\Delta J_c(X)$, the Fourier transform of $\Delta A(x)$ (5). The continuous intensity transform $\Delta J_c(X)$ is given by

$$\Delta J_c(X) = 2 \int_0^v \Delta A(x) \cos 2\pi Xx \, dx. \tag{7}$$

The intensity transform $\Delta J_c(X)$ for a particular value of v is computed from Eq. 7 and is then compared to the J_{obs} values using an agreement index AI where

$$AI = \frac{\sum_1^h | \Delta J_c(h) - J_{obs}(h) |}{\sum_1^h J_{obs}(h)}. \tag{8}$$

The AI values are obtained for a range of v values to determine the value of the parameter v precisely. If L were constant, with $d > 2v$, it follows from Eq. 7 that incorrect $\Delta J_c(X)$ values are obtained only when an estimate of v less than the correct value is made (5).

Deconvolution of the autocorrelation function $\Delta A(X)$ is carried out using either the recursion method or the relaxation method (5, 14). Two solutions $\pm s(x)$ for $\Delta t(x)$ are obtained but the $\pm$ ambiguity can be removed using density considerations (5), and the solution $+s(x)$ is correct for lipid bilayers. The recursion method is preferred to the relaxation method as it is much simpler to use (5). When a solution is obtained, namely, $s(x)$, then a test of the success of the deconvolution method is to compare the calculated and observed Fourier transform magnitudes. A comparison can be made using an agreement index, the R value, which is defined as

$$R = \frac{\sum_1^h || T_{obs}(h) | - | S(h) ||}{\sum_1^h | T_{obs}(h) |}, \tag{9}$$

where $S(X)$ is the Fourier transform of $s(x)$.

The solution $s(x)$ refers to $\Delta t(x)$, the electron density of the minus L model, and is a representation of the electron density of the lipid head group which has a width $v/2$. The calculation of the Fourier transform $s(x)$ provides a set of phases, denoted by $\{\pm\}$, for both models $\Delta t(x)$ and $t(x)$. The Fourier series representation for the lipid bilayer of electron density $t(x)$ is denoted by $t''(x)$ and

$$t''(x) = 2/d \sum_1^h \{\pm\} | T_{obs}(h) | \cos 2\pi hx/d. \tag{10}$$

A summary of the steps needed to obtain the electron density profile of the lipid bilayer is presented in Fig. 3. A brief account of this deconvolution method has been given previously (15).

At this stage in the structure determination there could easily be doubt about some of the phases for the reason that the R values are often larger than one might expect and also because the AI values often lead to a range of values for v. It is well known (1, 2) that the Fourier

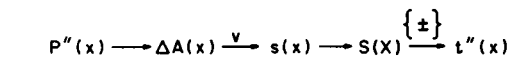

FIGURE 3 Flow chart for the direct analysis. The analysis is referred to as the zero-order analysis.

profiles $t''(x)$ for lipid bilayers generally show a dip in electron density centered at $x = \pm d/2$. This dip is associated with the meshing of the methyl groups at the end of the hydrocarbon chains. The minus L model with constant L is therefore an approximation to the true structure. An improved electron density model should include this dip in electron density. The dip in electron density is denoted by $q(x)$ and is transposed to $x = \pm d/2$, and we use the function $g(x)$ where

$$g(x) = q(x) * \delta(x - d/2), \tag{11}$$

with its origin at $x = d/2$ and

$$g(-x) = q(-x) * \delta(-x + d/2), \tag{12}$$

with its origin at $x = -d/2$. The improved minus L model is denoted $\Delta t_i(x)$ and for $0 \leq x \leq d/2$

$$\Delta t_i(x) = \Delta t(x) + g(x), \tag{13}$$

where the width of the $g(x)$ function is w and it is implied that $v > w$. A drawing of the improved minus L model is shown in Figure 4 A. The autocorrelation function of $\Delta t_i(x)$, the improved model, is complicated by the presence of the $g(x)$ function. The Patterson function $P_i''(x)$ of the improved model can be readily calculated and is given by

$$P_i''(x) = 2/d \sum_{1}^{h} \Delta J_i(h) \cos 2\pi hx/d, \tag{14}$$

where $\Delta J_i(h) = |\Delta T_i(h)|^2$ and where $\Delta T_i(X)$ is the Fourier transform of $\Delta t_i(x)$. The Patterson function $P_i''(x)$ is composed of three terms, namely B_1, B_{12}, and B_2 such that

$$P_i''(x) = B_1 + B_{12} + B_2. \tag{15}$$

The first term B_1 is

$$B_1 = \Delta A(x), \tag{16}$$

where $\Delta A(x)$ is defined by Eq. 4, and B_1 is centered at $x = 0$ and has a total width of $2v$. The third term, B_2, is

$$B_2 = g(x) * g(-x), \tag{17}$$

and is centered at $x = 0$ and has a total width of $2w$. The second term, B_{12}, is a cross-term and is given by

$$B_{12} = -2[g(x) * \Delta t(-x) + g(-x) * \Delta t(x)], \tag{18}$$

where B_{12} is centered at $x = \pm d/2$ and has a total width of $v + 2w$. The three terms B_1, B_2, and B_{12} of the Patterson function $P_i''(x)$ for the $\Delta t_i(x)$ model are illustrated in Fig. 4 B.

The improved model can be considered only after the steps outlined in Fig. 3 have been

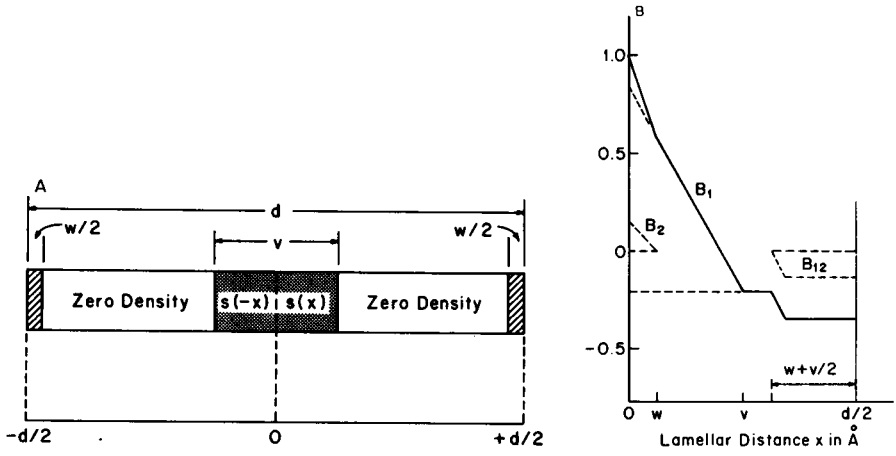

FIGURE 4 (A) The improved minus L model contains head group density $s(x)$ and zero density outside of the head group region but with a dip in electron density of width w centered at $\pm d/2$. (B) The Patterson function $P_i''(x)$ for the improved model $s(x) + g(x)$ is shown by the solid line. $P_i''(x)$ is composed of three terms: B_1 and B_2 are centered at $x = 0$, whereas B_{12} is centered at $d/2$. In the interval $0 \leq x \leq d/2$, B_1 has width v, B_2 has width w, and B_{12} has width $w + v/2$.

completed. This means that a first solution[1] $s_0(x)$ for the head group density has been obtained from $\Delta A(x)$ and an estimate of $g(x)$ has been obtained from the Fourier profile $t''(x)$. The improved model $\Delta t_i(x)$ is given by

$$\Delta t_i(x) = s_0(x) + g(x). \tag{19}$$

The first step in using the refined analysis is to obtain $\Delta A_1(x)$, the improved autocorrelation function of the head group density according to

$$\Delta A_1(x) = P''(x) - B_{12} - B_2. \tag{20}$$

The deconvolution of $\Delta A_1(x)$ using the recursion method provides $s_1(x)$, the electron density of the head group of the lipid molecule. The improved model at this stage is denoted $\Delta t_{i,1}(x)$ and

$$\Delta t_{i,1}(x) = s_1(x) + g(x). \tag{21}$$

The calculation of $\Delta T_{i,1}(X)$, the Fourier transform of $\Delta t_{i,1}(x)$, provides a set of phases $\{\pm\}$. The R value is obtained from Eq. 9 after substituting $\Delta T_{i,1}(h)$ for $S(h)$. The R value for the improved model should be considerably less than the R value for the first model.

A summary of the steps to obtain a new set of phases using the improved model is presented in Fig. 5. If the first set of phases $\{\pm\}$ derived from $S_0(X)$ is the same as the phases derived from $\Delta T_{i,1}(X)$, then, the Fourier profile $t''(x)$ is unchanged and the structure analysis is complete. However, unless the R value for $\Delta t_{i,1}(x)$ is quite small, it is safer to continue with another cycle of refinement until a minimum R value is obtained. On the other hand, if the second set of

[1]It is convenient to refer to the steps in Fig. 3 as the zero-order analysis. When the refined analysis is considered, the zero-order or the first solution is denoted $s_0(x)$ and its Fourier transform is denoted $S_0(X)$.

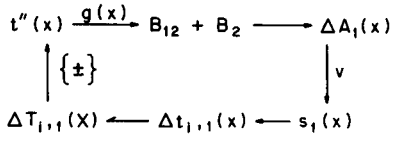

FIGURE 5

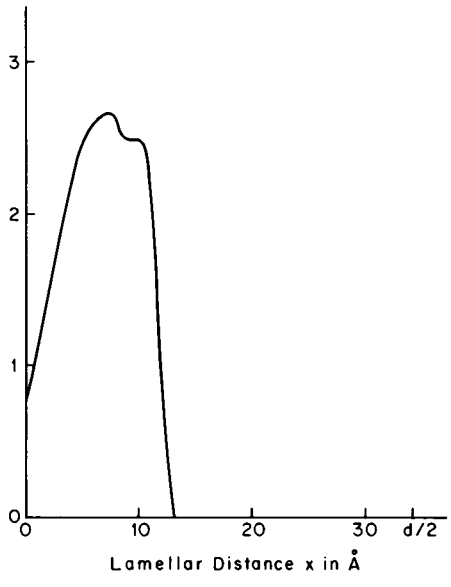

FIGURE 6

FIGURE 5 Flow chart for the refined analysis.
FIGURE 6 A hypothetical structure $m(x)$ which has zero density from $x = v/2$ to $x = d/2$.

phases are different from the first set obtained from $S_0(X)$, then additional cycles of refinement are necessary. After n cycles of refinement, the improved model is $\Delta t_{i,n}$ and

$$\Delta t_{i,n} = s_n(x) + g_{n-1}(x), \tag{22}$$

and the phases are obtained from $\Delta T_{i,n}(X)$, the Fourier transform of $\Delta t_{i,n}$.

STRUCTURE ANALYSIS

To demonstrate the feasibility of the present method and the operational procedures, the special case of a model structure is first considered. The deconvolution method is also used to derive phases for bilayers of phosphatidyl-ethanolamine (PE) and dipalmitoyl lecithin (DPC) using published data (9, 11, 16).

1. Model Calculations

A hypothetical structure which has a head group density from $x = 0$ to $x = v/2$ and zero density from $x = v/2$ to $x = d/2$ is considered. The electron density distribution $m(x)$ for the model structure with $v = 24.7$ Å and $d = 68.5$ Å is shown in Fig. 6. The X-ray data $d = 68.5$ Å, $h = 6$ are obtained from the model by computing $M(X)$, the Fourier transform of $m(x)$, at $X = h/d$, h an integer. The amplitudes $M(h)$ for $h = 6$ are listed in Table I.

The Patterson function $P''(x)$ is computed using Eq. 5 where the $|M(h)|^2$ values replace the $J_{obs}(h)$ values. The Patterson function $P''(x)$ for the model struc-

TABLE I

THE MODEL AMPLITUDES $M(h)$ AND THE AMPLITUDES $S(h)$ DERIVED USING DECONVOLUTION

h	1	2	3	4	5	6
$M(h)$	3.66	1.36	−0.82	−1.73	−1.28	−0.31
$S(h)$	3.65	1.53	−0.58	−1.60	−1.36	−0.50

ture is shown in Fig. 7. The choice of the v value can be made directly from the Patterson function for it is evident from Fig. 7 that $P''(x)$ is constant for $x \gtrsim 0.38\ d$, that is, $x \gtrsim 26$ Å. The choice of the v value can also be made by finding the minimum AI value as defined by Eq. 8. The continuous intensity transform $\Delta J_c(X)$ is computed using Eq. 7 for a range of v. AI values of 12, 1.5, and 1.8% were obtained for $v = 21.9$, 24.7, and 27.4 Å, respectively. A plot of $\Delta J_c(X)$ for $v = 24.7$ Å against $|M(h)|^2$ is shown in Fig. 8.

The autocorrelation function $\Delta A(x)$ is obtained from the Patterson function by

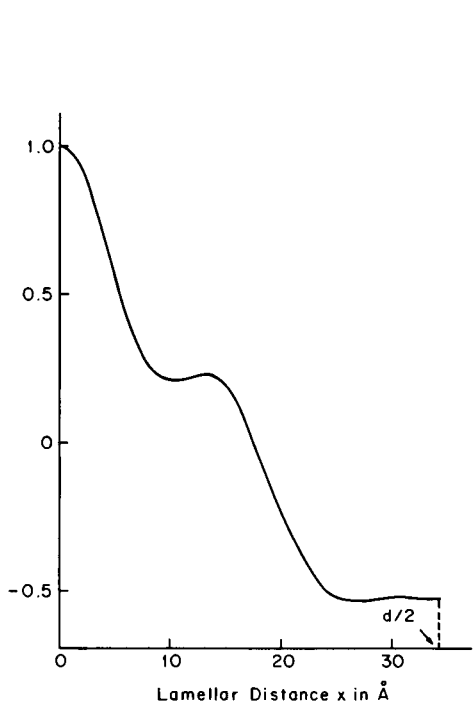

FIGURE 7

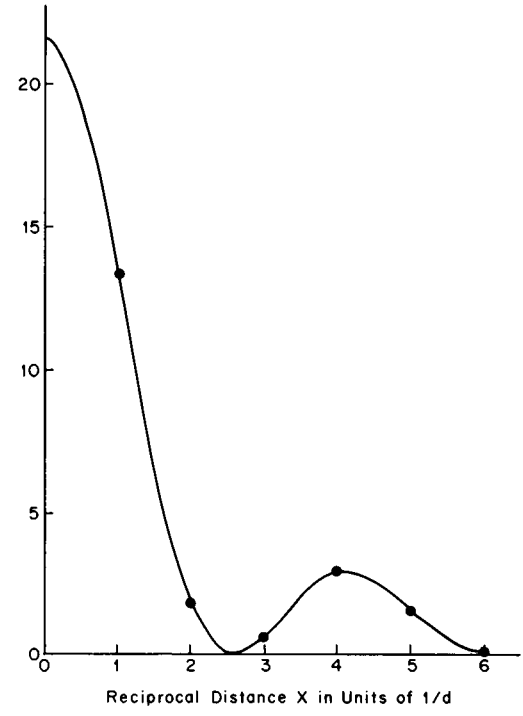

FIGURE 8

FIGURE 7 The Patterson function $P''(x)$ for hypothetical structure $m(x)$. The Patterson function is on a relative scale.

FIGURE 8 The intensity transform $\Delta J_c(X)$ for $v = 24.7$ Å is plotted as a function of h/d where $d = 68.5$ Å, the repeat period of $m(x)$. The model intensities $|M(h)|^2$ are shown as filled circles.

shifting the base line according to Eq. 6 and noting that $P''(v) = 0$ for the particular choice of v. The deconvolution of $\Delta A(x)$ is carried out using the recursion method. From diffraction theory (5, 14), an n-strip centrosymmetrical electron density model has a one-to-one correspondence with the autocorrelation function. The n-strip model of width v is divided into $2m$ equal strips of width δ and we use $\delta = d/50$. In the recursion method (5) the relationship between $m(x)$ and $\Delta A(x)$ is expressed by a m by m matrix involving m values of $\Delta A(v/2)$ to $\Delta A(v - \delta)$ and m values of the positive-half model defined in the interval $0 \leq x \leq v/2$. The solution $s(x)$ is obtained using the recursion relations generated by the m by m matrix (5). It is well known that the recursion method may not succeed. The primary reason is error propagation, for if errors are introduced via the end values $\Delta A(v - \delta)$ and $\Delta A(v - 2\delta)$, then these errors are magnified and propagated into successive values of $s(x)$. To test whether the solution $s(x)$ derived from $\Delta A(x)$ is the correct solution, a residual function $R(x)$ is calculated:

$$R(x) = s(x) * s(-x) - \Delta A(x). \tag{23}$$

An AI-type value is then calculated; this value is called the RT value and

$$RT = \frac{\Sigma \mid R(x) \mid}{\Sigma \mid \Delta A(x) \mid}, \tag{24}$$

where RT refers to recursion test and the summation is over the $2m$ values of the autocorrelation function. Note that Eq. 23 is the basic relationship in the deconvolution method and, moreover, the solution $s(x)$ which corresponds to the minimum $R(x)$ value is the correct solution. In the recursion method only one solution is obtained and there is no way to prove that $R(x)$ is the minimum. Ideally, all phase choices should be systematically examined as in the relaxation method (5, 13, 14). On the other hand, the recursion method has been previously used in a number of X-ray studies (4, 6, 7, 12, 16) to directly obtain the electron density structure.

The solutions $s(x)$ were determined using three values of v, v = 21.9, 24.7, and 27.4 Å. The Fourier transform $S(X)$ of $s(x)$ was computed at $X = h/d$, h an integer, in order that the phases of $S(h)$ and the R value could be determined. R values of 19.3, 8.8, and 60.8% for v = 21.9, 24.7, and 27.4 Å were obtained. The corresponding RT values were 2.1, 2.2, and a very large number. The recursion method worked efficiently for v = 21.9 Å and v = 27.4 Å but it failed for v = 27.4 Å for the reason that the end values were very small. In practice, the recursion method requires finite end values and it favors the minimum (correct) v value. The solutions obtained using v = 21.9 Å and v = 24.7 Å had the same phases for the first six reflections. The $S(h)$ values for v = 24.7 Å are listed in Table I. Some comment on the magnitude of the AI, RT, and R values is appropriate. It might be expected that all three values would be very close to zero but these values have a finite size, as noted elsewhere (13), because, in the computing, a finite strip width of $d/50$ is used.

In summary, the phases of the model structure $m(x)$ were directly found using the present method as described above. The method applies to any lipid bilayer structure

that has an approximately constant electron density in the hydrocarbon region and provided that $d \geq 2v$. It is wellknown (1–4) that there is a dip in electron density in the central part of the lipid chain region. The magnitude of this dip varies with the model membrane system (1–4). It is therefore instructive to consider a model structure that contains a dip in electron density at $x = \pm d/2$. The electron density of the modified model structure is denoted $u(x)$ and

$$u(x) = m(x) + g(x), \tag{25}$$

where $m(x)$ is the same as shown in Fig. 6 and where $g(x)$ is defined by Eq. 11 and $q(x)$ is a Gaussian function. The Gaussian function $q(x)$ is given by

$$q(x) = -ge^{-\pi(x/\beta)^2}, \tag{26}$$

where $q(x)$ has integral width β and g is the maximum dip expressed as a fraction of the maximum peak height of $m(x)$. In the refined analysis, the parameters g and β are estimated from the Fourier profile $t''(x)$ defined by Eq. 10. The Fourier transform of $u(x)$ is $U(X)$ and

$$U(h) = M(h) - (-1)^h g\beta e^{-\pi(h\beta/d)^2}. \tag{27}$$

The parameters g and β were arbitrarily assigned, and values of $U(h)$ for $h = 1$–6 were obtained from Eq. 27 and the $U(h)$ data set was then put on the same relative scale (10). The amplitudes $M(h)$ and $U(h)$ for $\beta = 5$ Å and g values of 0.23, 0.45, 0.68, and 0.90 are listed in Table II. The amplitude changes due to the dip in electron density $g(x)$ are dependent on g and β. The inclusion of a dip in electron density at $x = \pm d/2$ can lead to a phase change relative to $m(x)$ but these phase changes can only occur for the $h = 2, 3$, and 5 reflections.

Various model structures $u(x)$ with g values of 0.23, 0.45, 0.68, and 0.90 and β values of 3, 4, 5, 6, and 7 Å were considered. The amplitudes $U(h)$ were obtained from Eq. 27 and the Patterson functions $P''(x)$ were then computed. The continuous intensity transform $\Delta J_c(X)$ was computed for $v = 21.9$, 24.7, and 27.4 Å. For each model structure $u(x)$, with various g and β, the minimum AI value was $v = 24.7$ Å. The minimum AI value for the various model structures are listed in Table III. The

TABLE II

CALCULATED AMPLITUDES $M(h)$ FOR MODEL STRUCTURE $m(x)$ AND CALCULATED AMPLITUDES $U(h)$ FOR MODEL STRUCTURE $u(r)$ WITH A DIP IN ELECTRON DENSITY AT $x = \pm d/2$

g, β (Å)	h	1	2	3	4	5	6
0, 0	$M(h)$	3.66	1.36	−0.82	−1.73	−1.28	−0.31
0.23, 5	$U(h)$	3.96	1.08	−0.56	−1.96	−1.09	−0.47
0.45, 5	$U(h)$	4.25	0.80	−0.30	−2.19	−0.89	−0.63
0.68, 5	$U(h)$	4.55	0.52	−0.05	−2.42	−0.69	−0.80
0.90, 5	$U(h)$	4.84	0.24	+0.21	−2.65	−0.49	−0.96

The size and shape of the electron density dip is defined by parameters g and β.

TABLE III

AI VALUES FOR MODELS $u(x)$ WITH VARIOUS g, β VALUES

	β (Å)				
g	3	4	5	6	7
0.23	5.1	5.9	6.1	5.8	5.4
0.45	9.6	10.7	10.8	10.0	8.5
0.68	13.4	14.7	14.4	13.0*	10.7*
0.90	16.6	17.6*	16.9*	14.9*	12.1*

*One or, at most, two incorrect phases.

RT values increased from 6.0% for $g = 0.23$ and $\beta = 3$ Å to 12.1% for large g,β values. The *R* values showed a rapid increase from 10.3% for $g = 0.23$ and $\beta = 3$ Å to 52.0% for large g,β values. Correct phases were obtained for models with moderate g and β values as listed in Table III (values without an asterisk). Models with large g and β values (values with an asterisk) had one or, at most, two incorrect phases. The R values for the models $u(x)$ that gave the correct phases varied from 6.0% to a maximum value of 44.9%, whereas the models $u(x)$ that led to incorrect phases had R values of 47.3–52.7%.

So far, it has been demonstrated that the correct phases of models $u(x)$ with moderate g,β values can be directly determined. The models with large g,β values led to some incorrect phases. The correct set of phases can, however, be obtained by using the refined analysis which includes the effect of the dip of electron density at $x = \pm d/2$. The refined analysis is considered in the case of PE and DPC.

2. *Phosphatidyl-ethanolamine (PE)*

X-ray data $d = 49.5$ Å, $h = 15$ from oriented bilayers of PE have been reported by Hitchcock et al. (11). These authors have derived the phases of PE by drawing comparisons with the crystal structure of 1-2 dilauroyl-DL-PE (17). We restrict our analysis to the first five orders of diffraction. The observed X-ray data $|T_{obs}(h)|$ and the Fourier transform values from the molecular model $T_c(h)$ obtained by Hitchcock et al. (11) are listed in Table IV. The phases are relative to an origin at the interface of the head groups. The calculated model (11) had an R value of 14.3% for the first five orders.

The Patterson function $P''(x)$ for PE was computed using Eq. 5 and the X-ray data listed in Table IV. The Patterson function $P''(x)$ for $d = 49.5$ Å, $h = 5$, is shown in Fig. 9. The Patterson function shows a continuous fall-off until $v \approx 18$ Å and remains relatively uniform in the region 18 Å $\leq x \leq d/2$. The observed Patterson function in Fig. 9 resembles the ideal Patterson function in Fig. 2 A in that both are relatively uniform in the region $v \leq x \leq d/2$. From Fig. 9 the choice of $v \approx 20$ Å appears to be a reasonable one.

The correctness of the choice of v for obtaining the autocorrelation function $\Delta A(x)$ is further examined. The intensity transforms $\Delta J_c(x)$ for $v = 14$, 16, 18, and 20 Å were computed using Eq. 7. These transforms are plotted in Fig. 10

TABLE IV

THE OBSERVED $T_{obs}(h)$ AND CALCULATED $T_c(h)$ AMPLITUDES FOR PE* AND THE AMPLITUDES $S_0(h)$ AND $S_2(h)$ DERIVED FROM DECONVOLUTION USING THE ZERO-ORDER ANALYSIS AND TWO CYCLES OF REFINEMENT, RESPECTIVELY

h	1	2	3	4	5
$\lvert T_{obs}(h) \rvert$	3.49	0.53	0.65	1.36	0.27
$T_c(h)$	+3.48	+0.72	−0.09	−1.35	−0.60
$S_0(h)$	+3.30	+1.08	−0.80	−1.31	−0.66
$S_2(h)$	+3.46	+0.60	−0.67	−1.38	−0.32

*Reference 11.

together with the observed X-ray data $J_{obs}(h)$. The agreement index AI was computed using Eq. 3, and the AI values are listed in Table V. The choice of v = 20 Å has the lowest AI value.

The recursion method (5, 14) was used to deconvolute the autocorrelation function $\Delta A(x)$ using the four values of v. The solution $s(x)$ for v = 16 Å is illustrated in

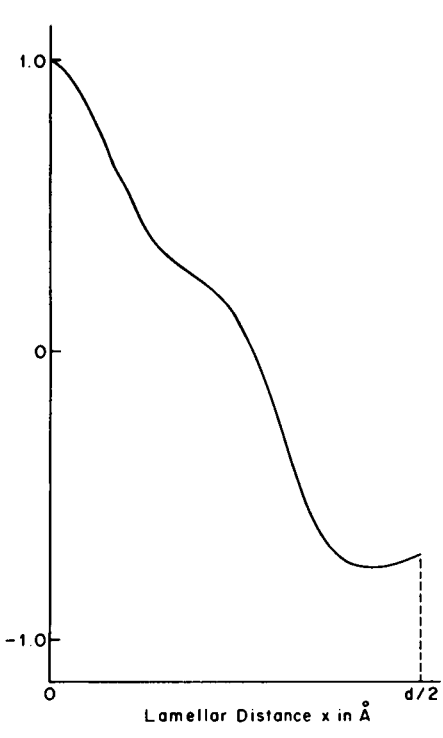

FIGURE 9

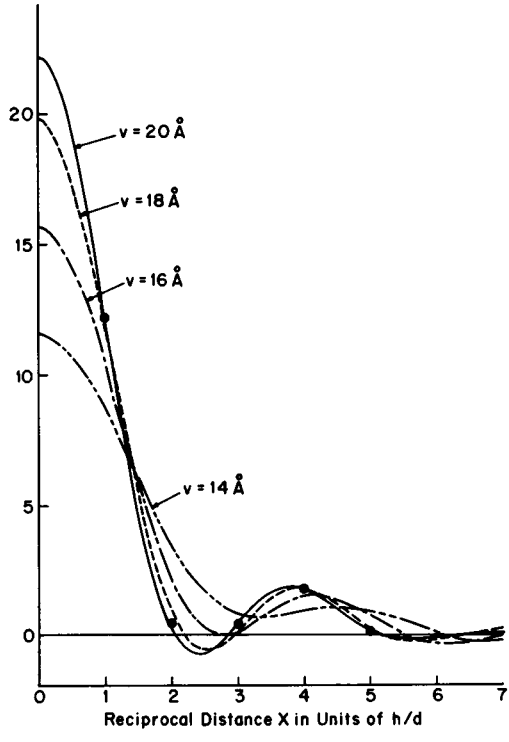

FIGURE 10

FIGURE 9 The Patterson function $P''(x)$ for PE was computed using the first five orders of diffraction of d = 49.5 Å. The Patterson function is on a relative scale.

FIGURE 10 The intensity transform $\Delta J_c(x)$ for four values of v is plotted as a function of h/d where d = 49.5 Å. The transforms refer to v = 20 Å (—), v = 18 Å (- - -), v = 16 Å (— - —), and v = 14 Å (—— - - ——). The observed intensities $J_{obs}(h)$ are shown as filled circles.

TABLE V

AI VALUES FOR FOUR VALUES OF v AND R VALUES FOR SOLUTION $s(x)$ USING THE SAME FOUR VALUES OF v.

v (Å)	14	16	18	20
AI (%)	60.1	34.3	10.7	2.3
R (%)	55.1	43.5	25.3	21.3

Fig. 11. The four solutions each had a maximum value between x = 4 Å and x = 8 Å. The Fourier transform $S(X)$ of the $s(x)$ function was computed for $X = h/d$, h an integer. The $S(h)$ values for v = 20 Å [denoted by $S_0(h)$] are listed in Table IV. The solutions for v = 16, 18, and 20 Å generated the same phases and these phases were the same as originally derived by Hitchcock et al. (11). On the other hand, the choice of v = 14 Å led to a different set of phases. The R values for the four values of v are listed in Table V. The choice of v = 20 Å gave the lowest R value of 21.3%, whereas the choice of v = 14 Å, which gave incorrect phases, had an R value of 55.1%.

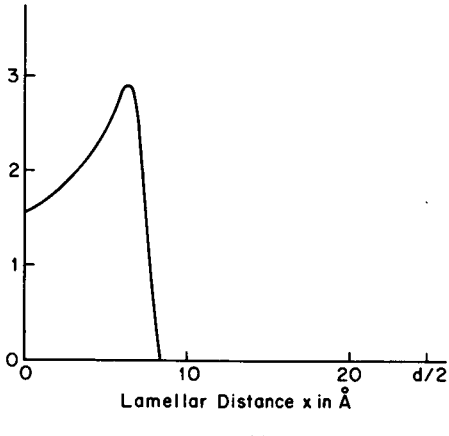

FIGURE 11

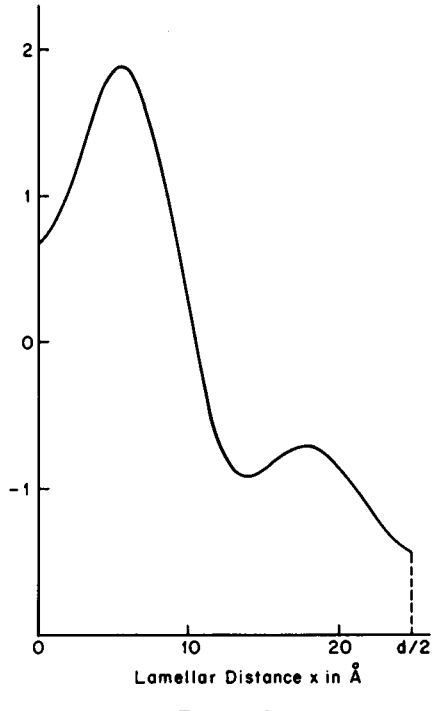

FIGURE 12

FIGURE 11 Solution $s(x)$ obtained by deconvolution using the recursion method for the case of v = 16 Å. The recursion method uses equal strips, and we have chosen a strip width of 0.99 Å. Thus $s(x) = 0$ for $x = 8.5\,(0.99) = 8.42$ Å (compare v = 16 Å).

FIGURE 12 Fourier series representation $t''(x)$ for PE computed using the first five orders of diffraction of d = 49.5 Å. The Fourier profile is on a relative scale and it has a resolution of about 5 Å.

The Fourier series representation of the PE bilayer is denoted $t''(x)$ and is given by Eq. 10. The Fourier profile $t''(x)$ was computed using the phases and the observed X-ray data in Table IV and is shown in Fig. 12. The resolution of the Fourier profile in Fig. 12 is 5 Å. The electron density of the head group has a maximum at x = 5 Å. It is evident that the electron density profile has a dip in electron density centered at $d/2$.

In summary the zero-order analysis of Fig. 3 using either v = 16, 18, or 20 Å gave the same set of phases but with R values ranging from 21.3 to 43.5%. It is instructive to proceed with the refined analysis outlined in Fig. 5 using the improved model $\Delta t_i(x)$ as defined by Eq. 19. The dip in electron density at $d/2$ is directly obtained from the Fourier profile in Fig. 12. The $g(x)$ function will be the same for the three choices of v (16, 18, and 20 Å) but the $\Delta t_i(x)$ models differ as the three solutions are slightly different. At this point in the analysis only the choices of v = 16 Å and v = 20 Å are studied. The improved model $\Delta t_i(x)$ for v = 16 Å is shown in Fig. 13.

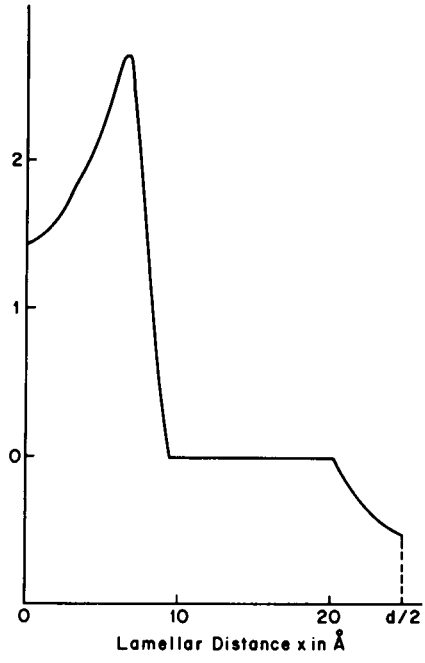

FIGURE 13

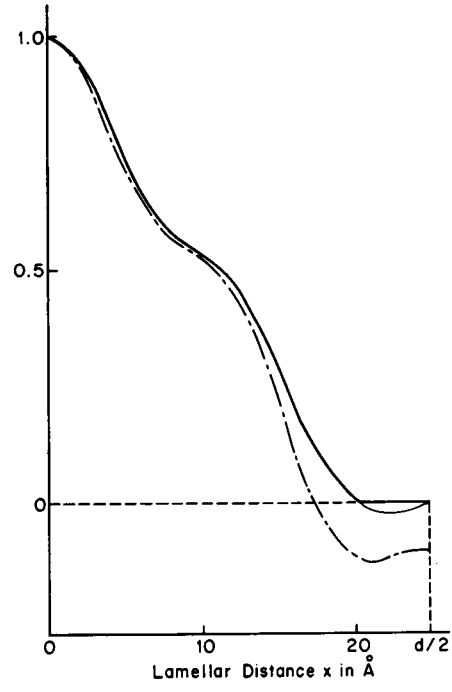

FIGURE 14

FIGURE 13 The improved electron density model $\Delta t_i(x)$ has $s(x)$ for the head group region, $g(x)$ for the dip in electron density centered at $d/2$, and zero density between $v/2 \leq x \leq (d - w)/2$. The solution $s(x)$ was obtained using v = 16 Å in the direct method.

FIGURE 14 The autocorrelation function $\Delta A_1(x)$ (—) which was obtained from the Patterson function $P''(x)$ (- —— -) after subtracting terms B_{12} and B_2 according to Eq. 20. The autocorrelation function is for the case of v = 16 Å . The base line for $\Delta A_1(x)$ is drawn in at v = 20 Å (actually at v = 20.3 Å because an equal number of strips of width 0.99 Å were used in the recursion method).

Note that, in practice, care was taken to underestimate the $g(x)$ function by a constant factor of about 20%. The R values for the two improved models $\Delta t_i(x)$ were computed using Eq. 9 after the Fourier transforms $\Delta T_i(X)$ of the models were evaluated. The R values are listed in Table VI (model 1) and they are already much lower, 34.1% for v = 16 Å and 11.1% for v = 20 Å.

The improved autocorrelation functions $\Delta A_1(x)$ were computed using Eq. 20 together with Eqs. 17 and 18. The autocorrelation function for v = 16 Å is shown in Fig. 14. The $\Delta A_1(x)$ curve for the v = 16 Å choice indicates that the correct choice of v is not 16 Å but is closer to 20 Å. Thus, in Fig. 14 the base line for $\Delta A_1(x)$ starts at x = 20 Å. The $\Delta A_1(x)$ curve for v = 20 Å also indicated that v = 20 Å was the correct choice.

The deconvolution of $\Delta A_1(x)$ for the two choices of v gave two solutions for $s_1(x)$. These solutions were combined to form a new model $\Delta t_{i,1}(x)$ after adding the $g(x)$ function according to Eq. 21. The Fourier transforms of the two choices were next calculated. The phases were the same as given by the first solution. the R values for the two choices after one refinement are listed, in Table VI (model 2), and they are now lower with R values of 9.6% for v = 16 Å and 4.6% for v = 20 Å.

A second cycle of refinement was tried. Two new autocorrelation functions $\Delta A_2(x)$ were obtained and both functions were relatively constant for x > 20 Å. The deconvolution gave two solutions $s_2(x)$ which were combined with $g(x)$ to give the $\Delta t_{i,2}(x)$ models. The R values are listed in Table VI (model 3) and are 4.0 and 3.1%, respectively. The phases derived from the $\Delta t_{i,2}(x)$ models were unchanged. The R values for the two original choices, v = 16 Å and v = 20 Å are plotted as a function of the cycle of refinement and are shown in Fig. 15. The zero-order analysis of Fig. 3 is indicated by 0 whereas the improved model is indicated by i and the $\Delta t_{i,1}(x)$ and $\Delta t_{i,2}(x)$ models refer to the 1 and 2 cycles of refinement, respectively. Values of g = 0.21 and w = 9.9 Å ($\beta \approx$ 5 Å) were used in the refined analysis.

3. *Dipalmitoyl Lecithin (DPC)*

A number of X-ray studies have been made on oriented bilayers of DPC at various humidities (1, 2). The swelling method was difficult to apply because the structure of DPC changes with swelling (9). Phases were, however, obtained and there is agree-

TABLE VI

R VALUES FOR IMPROVED MODELS USING TWO VALUES OF v

1. Model: $s(x) + g(x)$		
v (Å)	16	20
R (%)	34.1	11.1
2. Model: $s_1(x) + g(x)$		
v (Å)	20	20
R (%)	9.6	4.6
3. Model: $s_2(x) + g(x)$		
v (Å)	20	20
R (%)	4.0	3.1

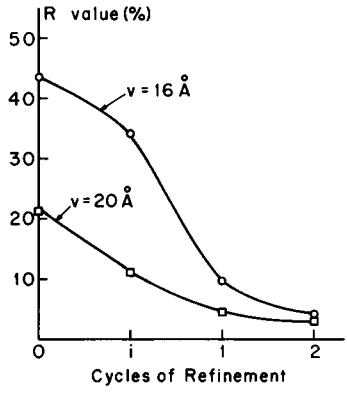

FIGURE 15 R values for the analyses using v = 16 Å and v = 20 Å. The direct method refers to zero cycles of refinement, the improved model $\Delta t_i(x)$ is indicated by i, the first and second cycles of the refined analysis are indicated by 1 and 2.

ment on the choice of phases of DPC at low humidity. The DPC phases were obtained in two different ways: as a result of finding a structure that gave the smallest changes on swelling (9) and by a deconvolution of the X-ray data from dispersions (16).

X-ray data (*a*) from DPC d = 55.5 Å, h = 6, reported by Lesslauer et al. (16) and X-ray data (*b*) from DPC d = 56.6 Å, h = 6, reported by Torbet and Wilkins (9) are considered. The $|T_{obs}(h)|$ values are listed in Table VII for the two data sets. Patterson functions were computed and AI values were obtained for a range of v. Well-defined minimum AI values were obtained: for data (*a*) an AI value of 17.7% was obtained for v = 20 Å (19.98 Å), whereas for data (*b*) the AI value was 13.3% for v = 20 Å (20.38 Å). The deconvolution led to $S_0(h)$ values and R values of 57.4% were obtained for data (*a*) and 40.2% for data (*b*). The $S_0(h)$ values for the two data sets are listed in Table VII. Both $S_0(h)$ values had the same set of phases (+, +, −, −, −, +) but this set of phases did not agree with the accepted phases (+, +, +, −, 0, −) derived in previous work (9, 16).[2]

The Fourier profiles for data sets (*a*) and (*b*) computed using the observed $|T_{obs}(h)|$ values and the $S_0(h)$ phases were quite similar to the published Fouriers obtained using the accepted phases (9, 16). In particular, the DPC bilayers showed a pronounced dip in electron density at $x = \pm d/2$. The g values were comparatively large in the range of 0.6 to 0.8 and w was about 9 Å (and $\beta \approx 4.5$ Å). From Table III it is to be expected that the AI values for DPC would be above 10%.

Two cycles of refinement were tried with data sets (*a*) and (*b*). The $S_2(h)$ values for data sets (*a*) and (*b*) are listed in Table VII. Both $S_2(h)$ values had the same set of phases (+, +, +, −, −, −) in agreement with the accepted set (9, 16). The data set (*a*) had an R value of 13.4% when using v = 18 Å (17.76 Å), g = 0.68, and

[2]Note that the DPC phases (9, 16) were originally given relative to the origin at the center of the hydrocarbon chain region. The phases quoted here are relative to the origin at the interface of the head groups. An origin shift of $d/2$ changes the signs of the odd orders but leaves the signs of the even orders unchanged.

TABLE VII

$S_0(h)$, $S_2(h)$, AND $T_{obs}(h)$ FOR DPC*

h	1	2	3	4	5	6
d = 55.5 Å (16)						
$\lvert T_0(h) \rvert$	4.25	0.19	0.27	2.31	0	1.00
$S_0(h)$	4.87	1.41	−1.03	−1.89	−1.14	0.12
$S_2(h)$	4.25	0.23	0.36	−2.28	−0.70	−0.80
d = 56.6 Å (9)						
$\lvert T_0(h) \rvert$	4.07	0.44	0.75	2.00	0	1.00
$S_0(h)$	3.95	1.41	−0.90	−1.70	−0.98	0.20
$S_2(h)$	4.15	0.23	0.50	−2.06	−0.44	−0.62

*Derived from deconvolution using the zero-order analysis and two cycles of refinement, respectively.

w = 8.9 Å. The data set (b) had an R value of 17.1% when using v = 18 Å (18.11 Å), g = 0.69 and w = 9.06 Å.

DISCUSSION

It has been demonstrated in the case of a model structure that the zero-order analysis worked efficiently at low resolution even when a moderate dip of electron density defined by g,β values was introduced. Even with values of $g \approx 0.6$ the zero-order analysis was successful.

In the X-ray analysis of PE the phases for the first five diffraction orders were derived and these phases remained unchanged during the 0, i, 1, 2 cycles of refinement. These phases are the same as the phases originally derived by Hitchcock et al. (11) using another method. The zero-order analysis of Fig. 3 sufficed to give the correct phases, whereas the refined analysis of Fig. 5 gave the same phases and much lower R values.

One reason why the present method worked efficiently with the PE bilayers is that PE has a relatively uniform hydrocarbon chain density and only a moderate central dip in electron density with g = 0.21 and $\beta \approx 5$ Å. Comparison between PE and the model calculations (Tables II and III) indicates that the zero-order analysis for PE is likely to succeed. This, however, assumes that $d \geq 2v$ and that the lipid chain region has uniform density apart from a central dip in electron density. It is also noted that the initial choice of v was not overly important for, in the refined analysis, the new autocorrelation function $\Delta A_i(x)$ tended to reveal the correct v.

In the X-ray analysis of DPC, phases for the first six diffraction orders were derived. DPC bilayers were not the best choice for the present method because the Fourier profiles (9, 16) show that the g,β values are comparatively large; values of $g \gtrsim 0.6$ and $\beta \approx 4.5$ Å were used in the refinement. The model calculations (Tables II and III) indicate that the success of the zero-order analysis would be borderline. In fact, the zero-order analysis gave two incorrect and four correct phases. The inclusion of the g,β values in the refined analysis led to the correct phases and gave moderately low R values after two cycles of refinement.

The zero-order analysis of Fig. 3 depends on the lipid bilayer having only moderate g,β values together with the requirement that $d \geq 2v$. Operationally, a v value that

lies within the correct range of values has to be chosen, but this presents no difficulty. The refined analysis of Fig. 12 is an extension of the zero order in that a new solution is obtained by deconvolution. The autocorrelation function from which the new solution is obtained uses information on the size and shape of the central electron density dip and this information is directly obtained from the Fourier profile. Thus, the refined analysis uses deconvolution and makes use of a cycle of refinement.

The present method applies to all lipid bilayers provided that $d \geq 2v$. This condition holds for nearly all lipid bilayers which contain very little water between the head groups. The validity of the method is based on the assumption that the lipid chain region has a uniform density. The uniform lipid chain density ensures that the Patterson function has a flat region from $x = v$ to $x = d/2$ and this is necessary for the deconvolution method. It has been demonstrated that the present method can also be used even when the bilayers have a pronounced central dip of electron density in the hydrocarbon region. The essential reason why the present method works for lipid bilayers with a central dip in electron density is that the Gaussian dip function $g(x)$ makes only a small contribution to the autocorrelation function in the region of deconvolution $x = v/2$ to $x = v$ (using the recursion method).

The present method was originally developed to derive the phases of model membrane systems that contain only a single lipid component (15), and it was first used to obtain the phases of sphingomyelin bilayers (18). The question whether the deconvolution method might work with lipid bilayers containing more than one component, either another lipid, cholesterol, or a protein component, cannot be easily answered at this time. It depends on the extent to which the additional components actually perturb the uniformity of the hydrocarbon chain region. If the uniformity is destroyed, the present method will not succeed because the autocorrelation function $\Delta A(x)$ cannot be isolated from the Patterson function. On the other hand, if there is only a moderate change in the uniformity of the hydrocarbon chain region then the deconvolution method is likely to succeed.

The question of whether the deconvolution method will yield correct phases at higher resolution has yet to be studied in detail. The determination of phases of the higher orders of diffraction from membranes has proven to be difficult (4) even when accurate X-ray data have been obtained. The recursion method is convenient but when higher order phases are studied it will probably be necessary to use the relaxation method so that all possible phase solutions can be examined (5, 13).

This work was supported by a grant from the U.S. Public Health Service.

Received for publication 10 June 1977 and in revised form 18 May 1978.

REFERENCES

1. SHIPLEY, G. G. 1973. Recent x-ray diffraction studies of biological membranes and membrane components. *In* Biological Membranes. Vol. 2. D. Chapman, editor. Academic Press, Inc., New York. 1–89.
2. LEVINE, R. K. 1972. Physical studies of membrane structure. *Prog. Biophys. Mol. Biol.* **24**:1.
3. MCINTOSH, T. J., R. C. WALDBILLIG and J. D. ROBERTSON. 1976. Lipid bilayer ultrastructure: elec-

tron density profiles and chain tilt angles as determined by x-ray diffraction. *Biochim. Biophys. Acta.* **448**:15.

4. WORTHINGTON, C. R. 1973. X-ray diffraction studies on biological membranes. *Curr. Top. Bioenerg.* **5**:1.
5. WORTHINGTON, C. R., G. I. KING, and T. J. MCINTOSH. 1973. Direct structure determination of multilayered membrane-type systems which contain fluid layers. *Biophys. J.* **13**:480.
6. LESSLAUER, W., and J. K. BLASIE. 1972. Direct determination of the structure of barium stearate multilayers by x-ray diffraction. *Biophys. J.* **12**:175.
7. LESSLAUER, W., J. CAIN, and J. K. BLASIE. 1971. On the location of 1-anilino-8-naphthalene sulphate in lipid model systems. *Biochim. Biophys. Acta.* **241**:547.
8. FRANKS, N. P. 1976. Structural analysis of hydrated egg lecithin and cholesterol bilayers. I. X-ray diffraction. *J. Mol. Biol.* **100**: 345.
9. TORBET, J., and M. H. F. WILKINS. 1976. X-ray diffraction studies of lecithin bilayers. *J. Theor. Biol.* **62**:447.
10. WORTHINGTON, C. R. 1969. The interpretation of low-angle x-ray data from planar and concentric multilayered structures. *Biophys. J.* **9**:222.
11. HITCHCOCK, P. B., R. MASON and G. G. SHIPLEY. 1975. Phospholipid arrangements in multilayers and artificial membranes: quantitative analysis of the x-ray diffraction data from a multilayer of 1-2-dimyristoyl-DL-phosphatidylethanolamine. *J. Mol. Biol.* **94**:297.
12. WORTHINGTON, C. R. 1973. X-ray analysis of retinal photoreceptor structure. *Exp. Eye Res.* **17**:487.
13. MCINTOSH, T. J., and C. R. WORTHINGTON. 1974. Direct determination of the lamellar structure of peripheral nerve myelin at low resolution (17 Å). *Biophys. J.* **14**:363.
14. HOSEMANN, R., and S. N. BAGCHI. 1962. Direct Analysis of Diffraction by Matter. North-Holland Publishing Co., Amsterdam. 734 pp.
15. KHARE, R. S., and C. R. WORTHINGTON. 1977. Direct structure determination of lipid bilayers. *Biophys. J.* **17**:50*a*. (Abstr.).
16. LESSLAUER, W., J. E. CAIN, and J. K. BLASIE. 1972. X-ray diffraction studies of lecithin bimolecular leaflets with incorporated fluorescent probes. *Proc. Natl. Acad. Sci. U. S. A.* **69**:1499.
17. HITCHCOCK, P. B., R. MASON, K. M. THOMAS, and G. G. SHIPLEY. 1974. Structural chemistry of 1-2-dilauroyl-DL-phosphatidylethanolamine: molecular conformation and intermolecular packing of phospholipids.
18. KHARE, R. S., and C. R. WORTHINGTON. 1976. The structure of oriented sphingomyelin bilayers. *Biophys. J.* **16**:137*a*. (Abstr.).